Dedicated to innovation in aerospace

NLR-TP-2022-176 | February 2023

Eddy current simulation and experiments for assessments of inductive heating in uni-directional thermoplastic composites

CUSTOMER: Clean Sky 2 Joint Undertaking

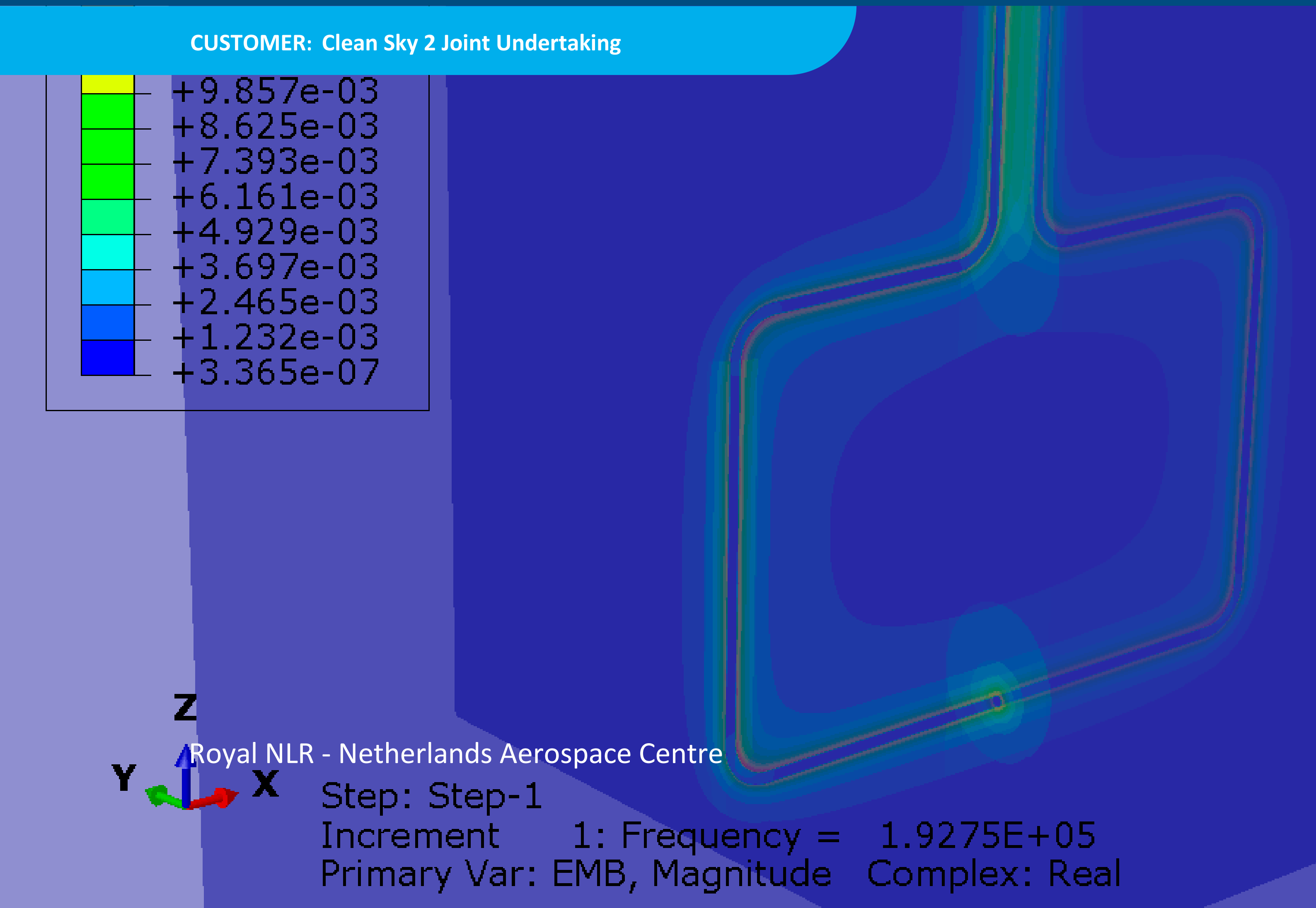

Royal NLR - Netherlands Aerospace Centre

Dedicated to innovation in aerospace

EXECUTIVE SUMMARY

UNCLASSIFIED

Eddy current simulation and experiments for assessments of inductive heating in uni-directional thermoplastic composites

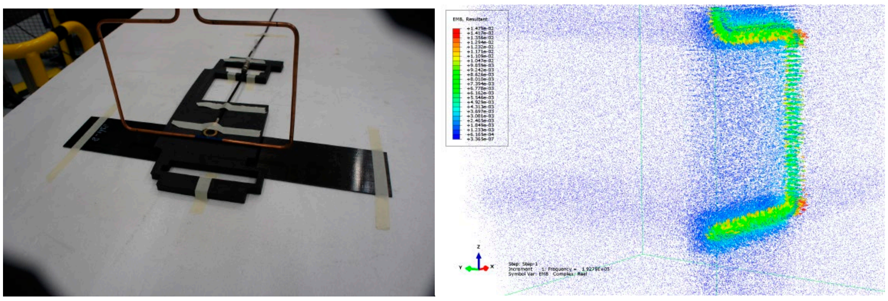

Figure 1: Left, magnetic field measurement test setup. Right, computed magnetic field surrounding the coil

Problem area

In the European R&D program Clean Sky 2, Large Passenger Aircraft Platform 2, a MultiFunctional Fuselage Demonstrator (MFFD) is developed that serves as a platform for examining the full potential of thermoplastic (TP) composites for the next generation of single aisle aircraft. Novel assembly techniques can contribute to weight reduction and automation of production. One such novel assembly technique is welding. This paper is focused more specifically on induction welding of thermoplastic uni-directional (UD) carbon fiber reinforced polymer (CFRP) materials.

Induction welding makes use of the fact that the thermoplastic matrix of TP composites can be re-melted by inductive heating, allowing TP composite adherends to be joined via welding. The inductive heating of woven fabric composites has been widely studied and reported. However, inductive heating of UD CFRP laminates is not well understood. To obtain confidence in the modelling approach and to have data available to compare simulation results with a realistic configuration that closely resembles induction welding equipment field measurements on a benchmark case are necessary such as shown in Figure 1.

REPORT NUMBER
NLR-TP-2022-176

AUTHOR(S)
A.J. de Wit
N. van Hoorn
L.S. Straathof
W.J. Vankan

REPORT CLASSIFICATION
UNCLASSIFIED

DATE
February 2023

KNOWLEDGE AREA(S)
Computational Mechanics and Simulation Technology
Aerospace Collaborative Engineering and Design
Structures and Manufacturing Technology

DESCRIPTOR(S)
Eectromagnetic
FEA
Magnetic field
Experiments
Validation

Description of work

A measurement setup has been developed to measure the current and voltage on the induction coil. Furthermore, a measurement setup has been developed to measure magnetic field lines near the induction coil that is attached to NLR's induction welding equipment. The magnetic field is measured near a coil hanging in free air, near a coil that is placed above an aluminium plate and near a coil that is placed above a composite plate. A 2D simplified numerical simulation model has been created that computes the magnetic field surrounding the coil and in addition computes the eddy currents generated inside an electrically conductive workpiece such as aluminium plate and composite plate. To capture 3D aspects in the electromagnetic field a 3D simulation model is created that models coil, surrounding air and workpiece.

Results and conclusions

The measured current and voltage were in good agreement with the input parameters used for the induction welding equipment. The measured field lines and the theoretical values for this type of setup agreed well. The 2D simulation model approached the theoretical and measured values very well for sufficient mesh refinement. The 3D model computed a good approximation to the measured field line values as the computational size of the model reached limits of the computer hardware capabilities. To carry out electromagnetic simulations with the current 3D simulation approach it is important to consider where to position the mesh refinement in order to strike a balance between model complexity and accuracy.

Applicability

The developed electromagnetic model for composite UD material can be used to support the power and frequency settings of an induction heating set-up for composite UD material. Furthermore, the measurement techniques developed can be used to measure magnetic field values near the coil. Via simulation of the inductive heating process an operator of an induction set-up can reduce the number of attempts to determine the ideal induction heating settings.

GENERAL NOTE
This report is based on a presentation held at the ICWAM 2022 International Congress on Welding, Additive Manufacturing and associated non-destructive testing, 8-9 June 2022 - Online.

Royal NLR
Anthony Fokkerweg 2
1059 CM Amsterdam, The Netherlands
p) +31 88 511 3113
e) info@nlr.nl i) www.nlr.nl

Dedicated to innovation in aerospace

NLR-TP-2022-176 | February 2023

Eddy current simulation and experiments for assessments of inductive heating in uni-directional thermoplastic composites

CUSTOMER: Clean Sky 2 Joint Undertaking

AUTHOR(S):

A.J. de Wit	NLR
N. van Hoorn	NLR
L.S. Straathof	NLR
W.J. Vankan	NLR

Royal NLR - Netherlands Aerospace Centre

This report is based on a presentation held at the ICWAM 2022 International Congress on Welding, Additive Manufacturing and associated non-destructive testing, 8-9 June 2022 - Online.

CUSTOMER	**Clean Sky 2 Joint Undertaking**
CONTRACT NUMBER	**945583**
OWNER	**NLR**
DIVISION NLR	**Aerospace Vehicles**
DISTRIBUTION	**Unlimited**
CLASSIFICATION OF TITLE	**UNCLASSIFIED**

APPROVED BY:		**Date**
AUTHOR	A.J. de Wit	30-01-2023
REVIEWER	S.M. Moghadasi	30-01-2023
MANAGING DEPARTMENT	A.A. ten Dam	30-01-2023

Summary

Induction welding of thermoplastic Carbon Fibre Reinforced Plastics (CFRP) is a fusion bonding technique that uses the possibility of the thermoplastic matrix to be re-melted to create a joint. Simulating this process with Finite Element Analysis (FEA) requires the modelling and numerical co-simulation of electromagnetic, thermodynamic, and mechanical aspects. Because of the complex physics involved, validating the numerical models is not straightforward and should include isolated experiments on separate physical phenomena. In this work, the validation of electromagnetic phenomena is considered. A technique is used to measure the magnetic field properties surrounding an induction coil representative of the induction welding equipment at NLR. The measurements are made around the coil and in proximity of a uni-directional (UD) ply CFRP laminate. The measured field properties are compared with the values that are computed via solving the electromagnetic field equations with FEA. The results of the experimentally obtained values and those calculated via FEA are in good agreement. Besides the magnetic field strength, also induced eddy currents were computed in the laminate, from which the joule heating was computed.

Contents

Abbreviations

ACRONYM	DESCRIPTION
AC	Alternating Current
CFRP	Carbon Fibre Reinforced Plastics
DC	Direct Current
EMF	Electro Magnetic Field
FEA	Finite Element Analysis
MFFD	MultiFunctional Fuselage Demonstrator
NLR	Royal NLR - Netherlands Aerospace Centre
TPCs	Thermoplastic Composites
UD	Uni-Directional

Eddy current simulation and experiments for assessments of inductive heating in uni-directional thermoplastic composites

A.J. de Wit[1*], N. van Hoorn[2†], L.S. Straathof[2†] and W.J. Vankan[1†]

[1*]Royal Netherlands Aerospace Centre - NLR , Anthony Fokkerweg 2, 1059 CM, Amsterdam, The Netherlands.
[2]Royal Netherlands Aerospace Centre - NLR, Voorsterweg 31, 8316 PR, Marknesse, the Netherlands.

*Corresponding author. E-mail: Bert.de.Wit@nlr.nl;
†Contributing authors: Niels.van.Hoorn@nlr.nl ; Luuk.Straathof@nlr.nl ; Jos.Vankan@nlr.nl;
†These authors contributed equally to this work.

Keywords: electromagnetic, FEA, magnetic field, experiments, validation, numerical simulation

Acknowledgments. This project has received funding from the Clean Sky 2 Joint Undertaking (JU) under grant agreement No 945583. The JU receives support from the European Union’s Horizon 2020 research and innovation programme and the Clean Sky 2 JU members other than the Union.

1 Introduction

For future single aisle aircraft the European R&D program Clean Sky 2, Large Passenger Aircraft Platform 2, is developing a Multi-Functional Fuselage Demonstrator (MFFD). Combinations of airframe structures, cabin/cargo, and system elements potentially enabling fuselage weight reduction, with high volume manufacturing methods and assembly methods at reduced recurrent costs, shall be validated through this MFFD [1]. For the assembly the development of advanced joining technologies and associated materials is necessary.

One example of such advanced joining techniques is induction welding of Thermoplastic (TP) CFRP materials. TP CFRPs can be re-melted allowing them to be joined via welding. Several mechanisms take part in constructing a successful induction weld. In this work we focus on one of the main mechanisms: the inductive heating part of the process.

The objective of our work is to develop 3D simulation models that provide the required insight into inductive heating for different material and geometric configurations. Because of the complexity of the underlying physics, our primary focus in this document is the measurement and computation of the magnetic field around a coil that captures the main aspects of dedicated induction welding tooling that is used at NLR.

This document can be read as follows. In Section 1.1 the background and underlying assumptions considered relevant for the present work are presented. In Section 2 the experimental measurements and a comparison with theoretical values are presented. In Section 3 a quasi-2D finite element model is presented that captures the main characteristics of the coil used in this work in the region where it is expected to generate a uniform electromagnetic field. This 2D model is then extended to a full 3D model of the coil and workpiece to capture 3D effects of the setup. In Section 4 some conclusions and directions for follow up research are given. In further work the authors intend to carry out thermal measurements with this setup to validate the thermal simulation of the inductive heating simulation.

1.1 Theoretical background

The complete physics behind induction heating is covered in e.g. [2]. In the present work the aspects considered relevant for the inductive heating process at NLR are highlighted.

Induction heating is accomplished by making use of the fact that the fibres in composite material are electrical conductors. By placing an electromagnetic coil close to a workpiece through which an alternating electric current flows a changing magnetic field is created and this magnetic field induces eddy currents within the workpiece, see Figure 2.

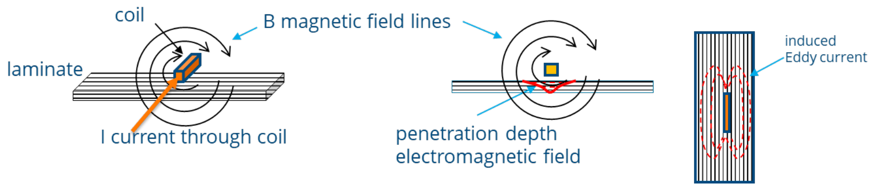

Figure 2: Eddy currents in a composite laminate due to induction coil [2]

For Eddy currents to occur, closed loops of electrically conductive paths are necessary. Hence, current flowing along fibres has to be able to return back along another set of fibres. If there is sufficient galvanic connection a conductive loop is created. Typically, in woven fabrics this is easily established as the fibres make contact in the weave. For Uni-Directional (UD) material this contact is not evident. Hence, UD material is typically more difficult to weld [3]. The Eddy currents cause resistive heating due to electric properties of the fibre material and the micromechanical structure of the laminate. Heating increases the temperature of the fibres bringing the surrounding polymer to the melting temperature.

For FEA simulation of the eddy currents, the magnetic vector potential is solved via electromagnetic analysis. Both electric and magnetic fields are computed in the entire domain (coil, workpiece and surrounding air). Hence, to obtain reference values that can be used to validate (part of) this FEA simulation the magnetic field strength is a suitable candidate which can be measured at fixed points from the coil. In [4] the authors have setup such a benchmark problem for a circular coil above an aluminium plate with a hole. In that work the magnetic field strength is measured between workpiece and coil. In the present work we've setup a similar experiment for the equipment at NLR which is outlined in the next section.

2 Experimental measurements

To obtain confidence in the numerical electromagnetic simulations measurements are performed that capture part of the computed values. In this work, the authors measure the magnetic field surrounding an induction coil in the presence of air, aluminium workpiece, and a composite workpiece. Before the measurements, the applied load is verified by measuring the current in the induction coil.

2.1 Experimental setup

Induction coils are designed with a specific application in mind. Therefore, many shapes and forms can be found for which different electromagnetic fields are constructed. In addition, the eddy currents that are generated in the workpiece are dependent on the coil shape and placement. Induction coils applied for studying inductive heating in composites, for instance Grouve et al. [5] Cheng et al. [6], usually have a different orientation and shape than the inductive heating equipment at NLR that was designed for welding long and slender structures.

To capture the main characteristics of the electromagnetic field a long slender coil is used that the authors expect to create a uniform field over a larger distance in the workpiece, see Figure 3a.

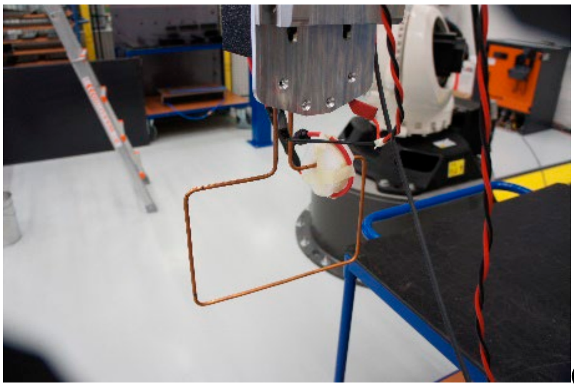
(a)
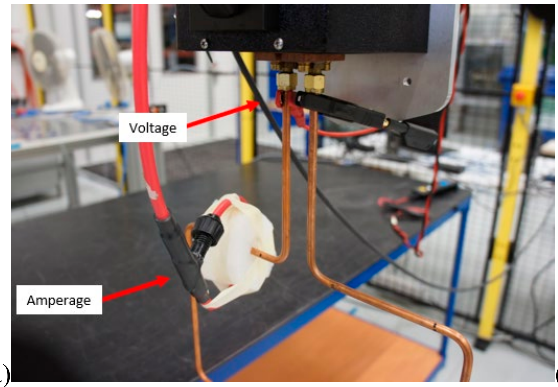

(b)

Figure 3: (a) Measurement of the Voltage. (b) Measurement of the Amperage applied to the coil

An operator of the induction equipment has the option to choose the coil amperage. Based on this amperage, the induction machine applies the most optimal frequency. It is unknown if the applied current matches the actual current in the coil. For electromagnetic simulations in Abaqus [7] it is necessary to confirm the current in the induction coil. Therefore, the amperage and voltage in the coil are measured with a setup as shown in Figure 3 (b).

After the current measurements the coil is placed on a Styrofoam table that does not interfere with the magnetic field. For measuring the magnetic field a probe is used. The circular probe is made of a non-magnetic material (i.e., brass) and therefore does not interfere with the magnetic field. The probe has an inner diameter of approximately 15 mm and a thickness of 5 mm. Using a known constant magnetic field the probe has been calibrated.

In order to measure the magnetic field close to the coil the magnetic field probe is positioned next to the coil as shown in Figure 4(a) and (b).

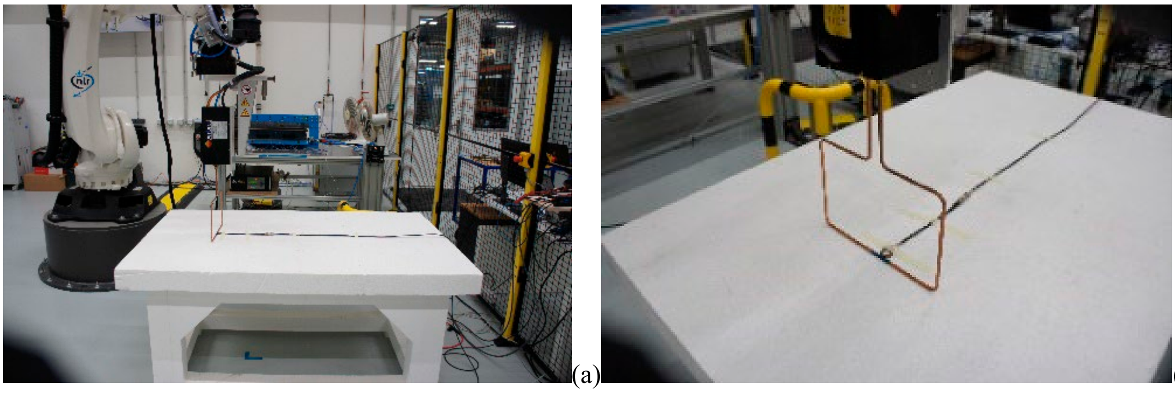
(a) (b)

Figure 4: (a) The test setup for measuring the magnetic field around the induction coil. (b) Coil used to measure the magnetic field surrounding the induction coil and workpiece

The probe is connected to an oscilloscope for data acquisition in the frequency domain. The magnetic field that is captured inside the magnetic field probe is measured.

For the measurements with aluminium plate and composite plate a nonconductive material is placed in between the coil and workpiece to fix the positioning of the field probe, see Figure 5.

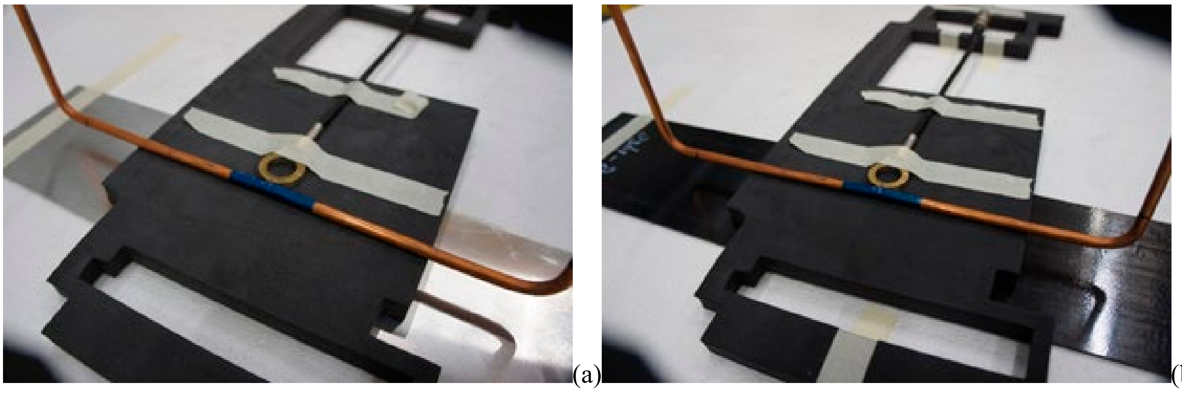
(a) (b)

Figure 5: Measurement of the magnetic field strength above the aluminium (a) and composite (b) plate

As a result, the coil and the probe have a constant spacing of 14 mm with the workpiece.

For the measurements in free air, with the aluminium plate, and with the composite plate the coil is moved horizontally in steps of 2 mm away from the probe. At each step the induction welding equipment is activated for two seconds to minimise heating of the workpiece. In this time, a measurement is taken and the frequency response from 100 kHz to 300 kHz is logged.

From basic electromagnetism theory, see Equation 1, it is known that magnetic flux density (B) decreases for increasing distance from the coil (r).

$$B = \frac{\mu_0 I}{2\pi r} \qquad (1)$$

Therefore, the magnetic field decreases within the probe inner diameter, which requires averaging of theoretical and simulated data for comparing the probe measurements in later sections. It is assumed that the magnetic field is uniform in the length direction of the coil and the simulation and theoretical data is averaged using a circular integral corresponding to the probe inner diameter.

2.2 Measurement results and discussion

The voltage and amperage measurements were performed prior to the magnetic field measurement. Here the input amperage was increased from approximately 50 A to 200 A. The measured RMS values of the amperage and voltage are listed in Table 1.

Table 1: RMS values of applied amperage and frequencies as measured

Input amperage [A]	Input frequency [kHz]	Measured RMS amperage [A]	Measured RMS voltage [V]
50.4	201	43.2	45.0
100.8	200	91.0	94.3
149.1	195	141.6	138.2
199.5	193	191.0	183.2

From Table 1 it is observed that the optimal frequency set by the induction welding equipment decreases for increasing amperage. This is because at higher amperages a lower frequency is required to obtain the same induction power. The measured RMS amperage is slightly lower compared to the input amperage. From the detailed time response of the amperage signal it is observed that variations in time could be the cause of these differences.
For the magnetic field measurements an input amperage of 199.5 A at 193 kHz is used. The accuracy of the magnetic field measurements is determined by comparing the theoretical values of the magnetic field strength with the measured values, see Figure 6. Here the theoretical values are averaged over the probe inner diameter as explained in Section 3.1.

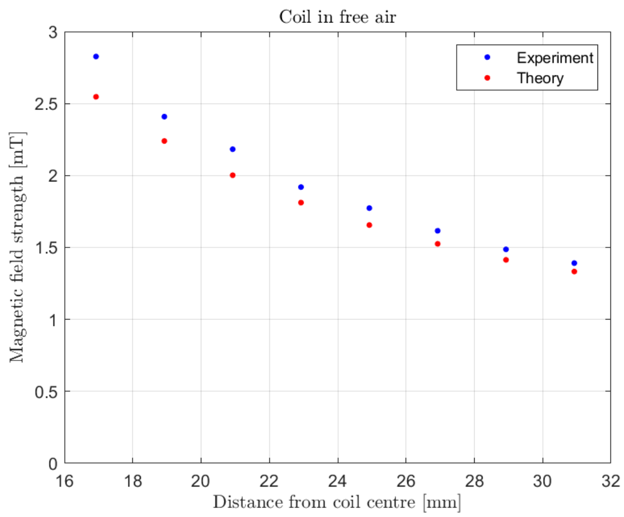

Figure 6: Magnetic field strength measured and the theoretical value

The results are in good agreement and follow the same trend. A difference of 4% to 11% between the theory and the experiment is observed for each measurement. There are several aspects that could be the cause of this difference. Firstly, the theory is based on Direct-Current (DC) while for the experiment Alternating-Current (AC) at a relatively high frequency is used. Secondly, the probe is calibrated in a constant AC magnetic field that differs from the varying magnetic field. Despite theoretically correct averaging of the theoretical data over the inner area of the probe this could differ from reality. Thirdly, a slight position inaccuracy of the probe (e.g., in the order of 0.5 mm) will

significantly affect the result, especially for the measurements closest to the coil. Because the coil that was used to measure the magnetic field strength has a certain thickness the measurements could not be conducted closer to the coil than 17[mm].
The results of the magnetic flux density measurements involving a workpiece close to the coil, i.e. aluminium plate and composite plate are shown for each measurement in Figure 7.

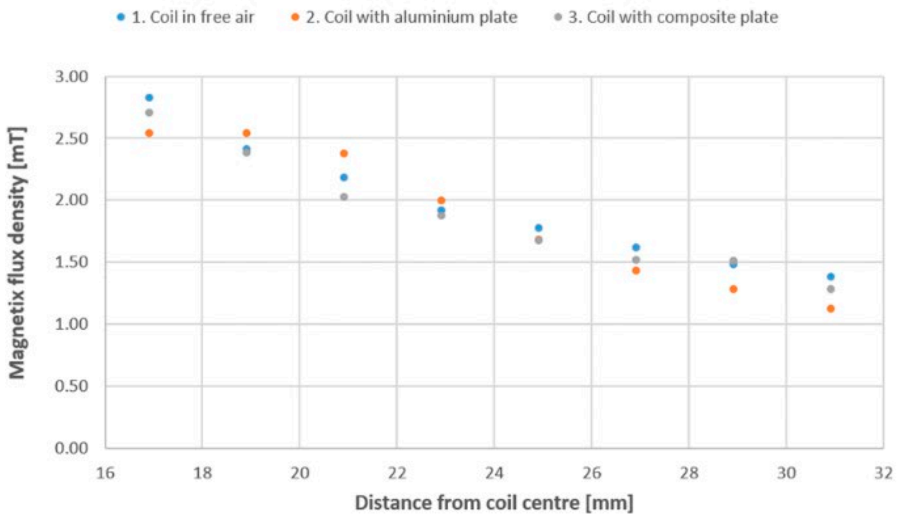

Figure 7: Magnetic field strength measured at a distance from the coil

The measurements in air and with a composite workpiece are in good agreement. As can be expected the composite plate has an negligible effect on the magnetic field. Measurements shown for the aluminium plate are lower than expected closer to the coil. The reason has not been determined but may be due to the averaging that was used to compute the measurement values.

3 Numerical simulation model

In this work the Finite Element package Abaqus [7] is used for the electromagnetic modelling. Derivation of the underlying equations can be found in the theory manual. Here we focus on the relevant steps to create the analysis model.

3.1 2D Model geometry and boundary conditions

To capture the magnetic field between coil and workpiece a quasi 2D model is created that covers the centre section of the coil as highlighted in Figure 8(a).

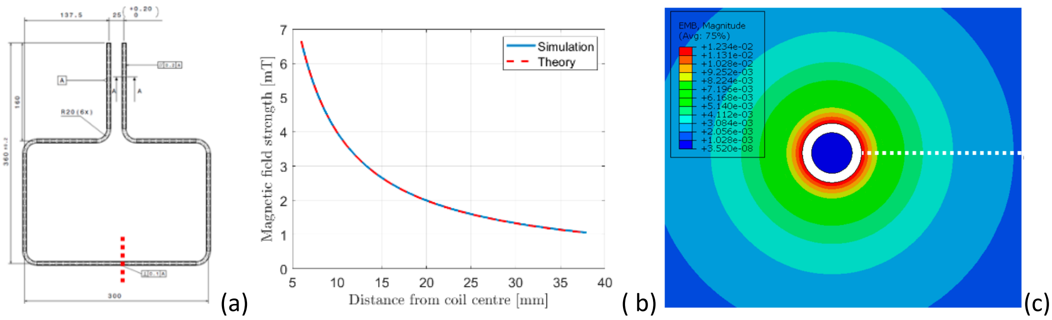

Figure 8: (a) Geometry of the coil and the modelled section where the 2D model is created. (b) The 2D abaqus model results coincide with the theoretical field values. (c) Contour plot of the simulated magnetic field and a dashed white line indicates where the field values are taken

The coil inner radius is 2.175 mm and outer radius is 3.175 mm. The distance between the bottom of the coil and the workpiece is 14 mm. The aluminium workpiece has a thickness of 2 mm and the composite workpiece has a $[0/90]_{8s}$ layup. Each ply is 0.138 mm thick and the total thickness equals 2.208 mm. The width of the workpiece is 100 mm. The air surrounding coil and workpiece is a 210x210 mm box. Because 3D elements are used the thickness of the model is set to 0.138 mm.
The mesh density is chosen to include 4 elements in ply thickness direction and a total of 26446 nodes of 12998 EMC3D8 elements. The 2D simulation model is shown in Figure 9.

Figure 9: 2D model showing the induction coil(white) and workpiece (red) surrounded by air (green).

The material properties used for the FEA model for air, coil and workpiece are listed in Table 2.

Table 2: Material properties used in the modelling

	Electric conductivity [S/m]	Magnetic [H/m]	Dielectric constant [-]
Air	1.0	1.2566E-06	8.85419E-12
Coil	1.0	1.2566E-06	8.85419E-12
Aluminium	37700000	1.2566E-06	8.85419E-12
C/PEKK [5]	22900	1.2566E-06	8.85419E-12
	3.37		
	0.4		

The values for electric conductivity of air and coil are set to 1 S/m corresponding to low conducting regions. The coil conductivity is set to 1 S/m to prevent calculating eddy currents in this region that would oppose the applied current to the coil. The interested reader is referred to the Abaqus documentation [7] for an explanation.

The values computed by Abaqus are compared with theoretical values as plotted in Figure 8(b). As can be seen there is good agreement between the theoretical value and the computed solution. Furthermore, the computed values of the magnetic field strength are compared with the experimentally obtained values in Figure 10(a-c).

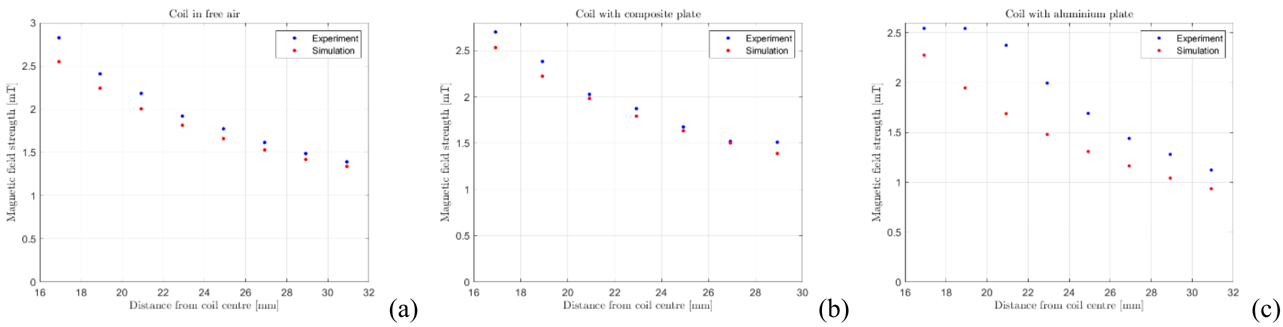

Figure 10: Computed 2D simulation results for the magnetic field strength compared with the measurements

For the coil in free air (Figure 10(a)) and the composite plate (Figure 10(b)) the results are in good agreement. For the coil with the aluminium plate (Figure 10(c)) there is a larger difference closer to the coil. The reason has not been determined but could be an incorrect measurement.

3.2 3D Model geometry and boundary conditions

To capture 3D effects of the induction setup a 3D FEA model is constructed. The FEA model consists of 1/4th of the geometry to reduce computation effort, see Figure 11(a).

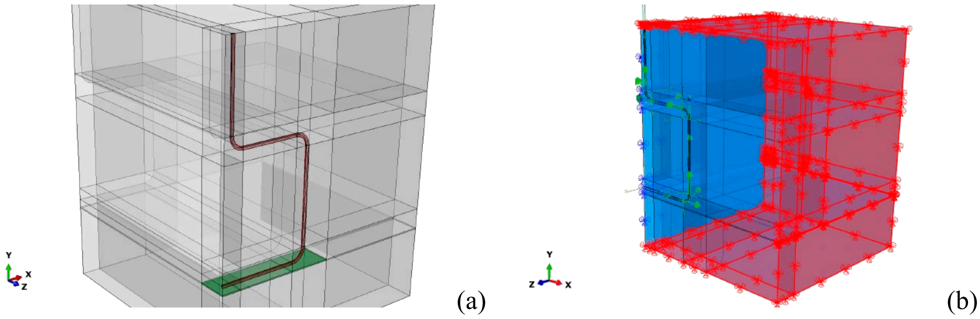

Figure 11: (a) 3D model of 1/4th of the geometry. In green the workpiece, in red the coil and in grey the air surrounding the setup. (b) Magnetic flux boundary condition set at the external surfaces

The air is modelled as a 400x400x500 mm box in which the coil and (when applicable) workpiece are placed. The workpiece is modelled as a (lxw) 200x50 mm plate that has a 2 mm thickness for the aluminium plate and a 16x0.138 mm thickness for the composite plate. For the composite plate the plies are modelled individually with an interface model [8]. The applied load corresponds to 1.18697E+07 A/m2 at a frequency of 192750 Hz. On the external surfaces the magnetic field strength is set to zero, see Figure 11(b). Neumann boundary conditions are set on the X-Y interface (see Figure 11(a)) and Dirichlet boundary conditions on the Y-Z interface (see Figure 11(a)). The mesh consists of 1.2M EMC3D8 elements with 1.27M nodes.

A contour plot of the magnetic field strength that is calculated is shown in Figure 11(a). In this plot the 1/4th model is mirrored to show the complete magnetic field strength surrounding the coil.

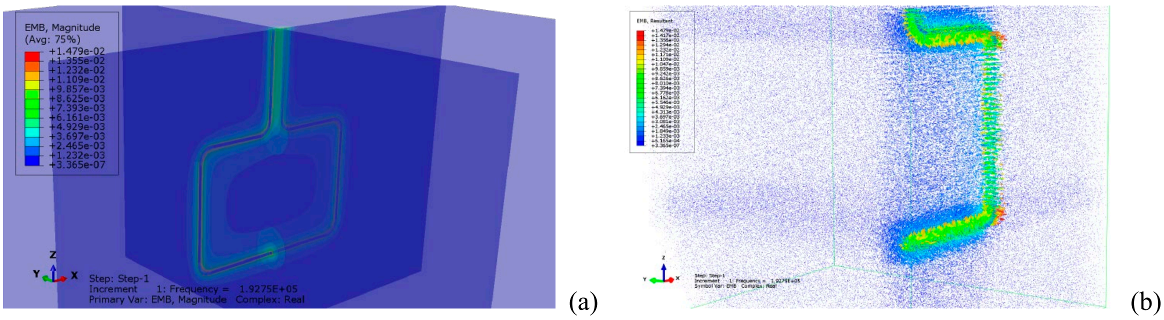

Figure 12: (a) Contour plot of the magnetic field around the coil.(b) Vector plot of the magnetic field around the coil 1/4th of the model

In Figure 12(b) a vector plot of the magnetic field is shown. The model covers only 1/4th of the coil corresponding to the Abaqus model. As can be seen from both plots the magnetic field strength decreases rapidly further away from the coil. In addition, below the coil a relatively uniform field is computed. Hence, this coil geometry is suitable to study a workpiece in a relatively uniform magnetic field.

The magnetic field strength of the 3D simulation can be compared with the 2D simulation in Figure 13 to determine the accuracy of the 3D model.

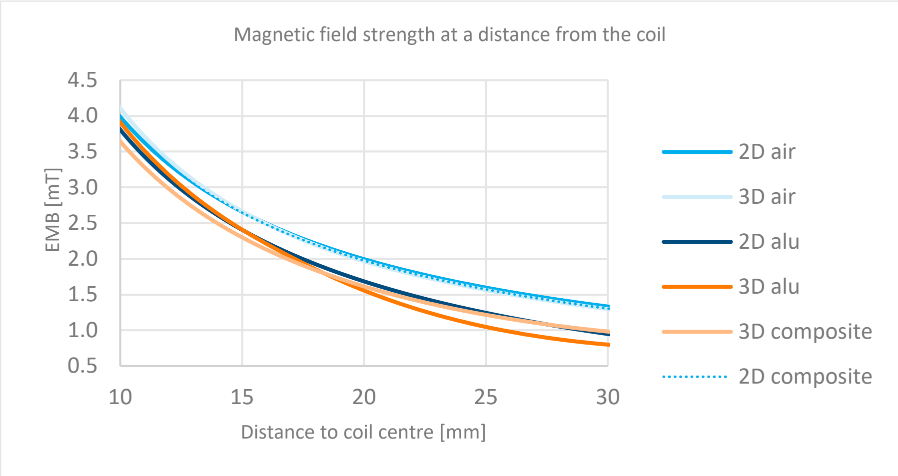

Figure 13: Magnetic field strength computed at a distance from the coil for both the 2D and 3D simulations

The computed magnetic field strength for the coil in air for both the 2D and 3D model are in good agreement. For the aluminium workpiece the magnetic field strength computed for both the 2D and 3D model are in good agreement as well. For the composite model the difference is larger. The reason for this is that the composite model uses 2 elements in thickness direction per ply. In addition, the interface model that is added introduces another 2 elements per ply interface. The mesh that results from this consisted of 2.5M elements where the authors hit the boundary of the computer architecture where this model was running. Hence, for 3D simulations a detailed modelling of the composite is only possible when the uniform part of the bottom of the coil is considered and the top part is excluded from the simulations.
For completeness, the eddy current density that is calculated in the aluminium plate is plotted in Figure 14.

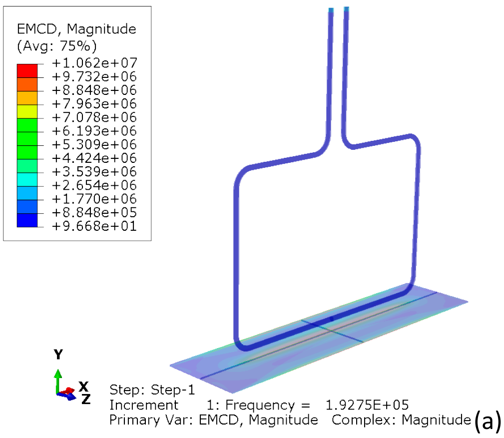

Figure 14: Eddy current density contour plot for the complete coil and workpiece geometry

The contour plot shows that below the coil the highest eddy current density is computed, but due to the slenderness of the workpiece the edges also show an increase in eddy current density. This effect is highlighted in Figure 15(a) for the eddy current density and in Figure 15(b) for the Joule Heating that is computed.

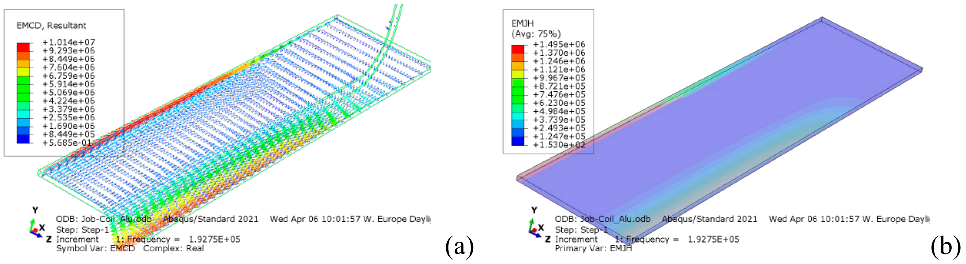

Figure 15: (a) Eddy current vector plot of the aluminium workpiece (1/4th model). (b) The joule heating computed for the aluminium workpiece (1/4th model)

For the sake of completeness the composite workpiece eddy current density is plotted in Figure 16(a) and the computed Joule heating in Figure 16(b).

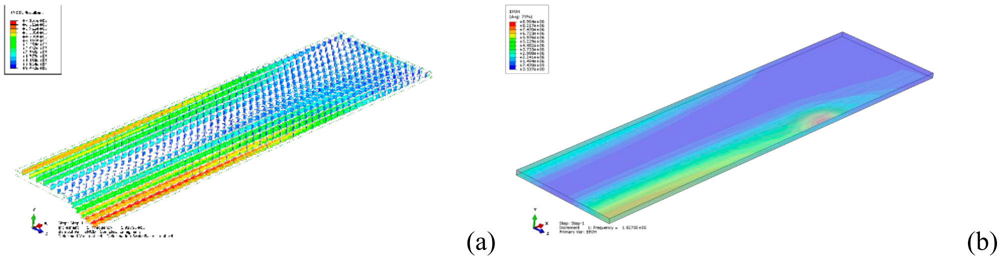

Figure 16: (a) Eddy current density composite workpiece (1/4th model). (b) The joule heating computed for the composite workpiece (1/4th model)

As can be seen from Figure 16 (a) the eddy current flow is largely the same pattern as could be seen for the aluminium plate. However, the Joule heating that is computed shows a difference in pattern where a hotspot is visible further away from the centre. The reason could be due to the anisotropy of the composite lay-up as shown in the eddy current density contour plot shown in Figure 17.

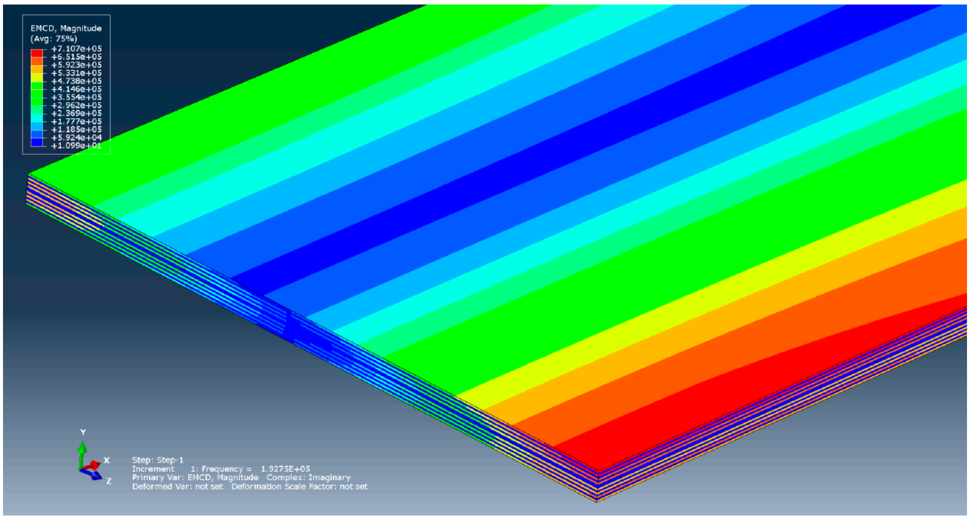

Figure 17: Zoom in of the composite plate contour plot of calculated eddy current density. The plies that are in the direction of the coil have a high current density and the cross-plies a low eddy current density

However, this is part of ongoing research as a temperature measurement of the current setup was out of scope and will be done in a follow up study.

4 Discussion and conclusion

In this work the authors present a measurement technique for measuring the magnetic field around an induction coil. This magnetic field was successfully measured and calculations using FEA showed good agreement with the measurement data. Furthermore, a measurement technique is presented to verify the amperage that is applied to the induction coil used in this study. This is important to accurately set the applied load to the Finite Element simulation model. In addition to magnetic field computations, the induced eddy currents were computed in the workpieces and from these eddy currents the joule heating was computed. The results of the Joule heating in the composite material show hot spots that could be due to the anisotropy of the material and that will be further investigated with thermal imaging in a follow up study.

5 Bibliography

[1] S. Veldman, P. Kortbeek, P. Wolcken, R. Herrmann, J. Kos en I. Fernandez Villegas, „Development of a multifunctional fuselage demonstrator,” in *Proceedings of Aerospace Europe Conference*, Bordeaux, France, 2020.

[2] C. Christopoulos, An Introduction to Applied Electromagnetism, Chichester: Wiley, 1990.

[3] P. Mitschang, M. Neitzel en R. Rudolf, „Induction heating of continuous carbon-fibre-reinforced thermoplastics,” *Composites Part A: Applied Science and Manufacturing,* pp. 1191-1202, 2000.

[4] K. Fujiwara en T. Nakata, „Results for Benchmark problem 7(Asymmetrical Conductor with a hole),” *International Journal for Computation and Mathematics in Electrical and Electronic Engineering.,* vol. 9, nr. 3, pp. 137-154, 1993.

[5] W. Grouve, E. Vruggink, F. Sacchetti en R. Akkerman, „Induction heating of UD C/PEKK cross-ply laminates,” in *23rd International Conference on Material Forming*, 2020.

[6] J. Cheng, B. Wang, D. Xu, J. Qiu en T. Takagi, „Resistive loss considerations in the finite element analysis of eddy current attenuation in anisotropic conductive composites,” *NDT and E International,* nr. 119, 2021.

[7] Simulia, Abaqus 2021 theory manual, Dassault Systèmes Simulia Corp., 2021.

[8] A. de Wit, N. van Hoorn, B. Nahuis en W. Vankan, „Numerical simulation of eddy current generation in uni-directional thermoplastic composites,” in *20th European Conference on Composite Materials*, Lausanne, 2022.

[9] T. Ahmed, D. Stavrov, H. Bersee en A. Beukers, „Induction welding of thermoplastic composites - an overview,” *Composites Part A: applied science and manufacturing,* pp. 1638--1651, 2006.

[10] H. J. Kim, S. Yarlagadda, N. B. Shevchenko, B. K. Fink en J. W. Gillespie Jr., „Development of a Numerical Model to Predict In-plane Heat Generation Patterns During Induction Processing of Carbon Fiber-reinforced Prepreg Stacks,” *Jounral of composite materials,* vol. 37, nr. 16, pp. 1461-1483, 2000.

[11] P. G. O'Shaughnessey, M. Dubé en I. F. Villegas, „Modeling and experimental investigation of induction welding of thermoplastic composites and comparison with other welding processes,” *Journal of composite materials,* vol. 50, nr. 21, pp. 2895--2910, 2016.

[12] X. Xu, H. Ji, J. Qiu, J. Cheng, Y. Wua en T. Takagi, „Interlaminar contact resistivity and its influence on eddy currents in carbon fiber reinforced polymer laminates,” *NDT and E International,* pp. 79-91, 2018.

[13] A. de Wit, N. van Hoorn, R. Nahuis en W. Vankan, „Prediction of thermo-mechanic effects through numerical simulation of induction heating of thermoplastic composites,” Royal Netherlands Aerospace Centre - NLR, Amsterdam, 2021.

Dedicated to innovation in aerospace

Royal NLR - Netherlands Aerospace Centre

NLR operates as an objective and independent research centre, working with its partners towards a better world tomorrow. As part of that, NLR offers innovative solutions and technical expertise, creating a strong competitive position for the commercial sector.

NLR has been a centre of expertise for over a century now, with a deep-seated desire to keep innovating. It is an organisation that works to achieve sustainable, safe, efficient and effective aerospace operations.
The combination of in-depth insights into customers' needs, multidisciplinary expertise and state-of-the-art research facilities makes rapid innovation possible. Both domestically and abroad, NLR plays a pivotal role between science, the commercial sector and governmental authorities, bridging the gap between fundamental research and practical applications. Additionally, NLR is one of the large technological institutes (GTIs) that have been collaborating over a decade in the Netherlands on applied research united in the TO2 federation.

From its main offices in Amsterdam and Marknesse plus two satellite offices, NLR helps to create a safe and sustainable society. It works with partners on numerous programmes in both civil aviation and defence, including work on complex composite structures for commercial aircraft and on goal-oriented use of the F-35 fighter. Additionally, NLR helps to achieve both Dutch and European goals and climate objectives in line with the Luchtvaartnota (Aviation Policy Document), the European Green Deal and Flightpath 2050, and by participating in programs such as Clean Sky and SESAR.

For more information visit: **www.nlr.org**

Postal address
PO Box 90502
1006 BM Amsterdam, The Netherlands
e) info@nlr.nl **i)** www.nlr.org

Royal NLR
Anthony Fokkerweg 2
1059 CM Amsterdam, The Netherlands
p) +31 88 511 3113

Voorsterweg 31
8316 PR Marknesse, The Netherlands
p) +31 88 511 4444